

# Loading quantum dots into thermo-responsive microgels by reversible transfer from organic solvents to water†‡

Lei Shen,<sup>ab</sup> Andrij Pich,<sup>ac</sup> Daniele Fava,<sup>a</sup> Mingfeng Wang,<sup>a</sup> Sandeep Kumar,<sup>a</sup> Chi Wu,<sup>bd</sup> Gregory D. Scholes<sup>\*a</sup> and Mitchell A. Winnik<sup>\*a</sup>

Received 28th August 2007, Accepted 19th December 2007

First published as an Advance Article on the web 15th January 2008

DOI: 10.1039/b713253k

We describe a new method for the preparation of fluorescent inorganic-nanoparticle composite microgels. Copolymer microgels with functional pendant groups were transferred *via* dialysis into tetrahydrofuran (THF) solution and mixed with colloidal solutions of semiconductor nanocrystals (quantum dots, QDs). CdSe QDs stabilized with trioctylphosphine oxide (TOPO) became incorporated into the microgels *via* ligand exchange of pendant imidazole (Im) groups for TOPO. PbS QDs stabilized with oleic acid were incorporated into microgels with pendant –COOH groups. This approach worked equally well with microgels based upon poly(*N*-isopropylacrylamide) (PNIPAM) and those based upon an acetoacetyethyl methacrylate-*N*-vinylcaprolactam copolymer (PVCL). These composite hybrid materials were colloidally stable in THF, and maintained their colloidal stability after transfer to water, either *via* dialysis or by sedimentation–redispersion. In water, the composites exhibited similar thermal responsiveness to the parent microgels, with a small shift to lower temperature in the volume phase transition. This approach allows one to use inorganic nanoparticles synthesized under optimum conditions in organic media at high temperature and to prepare composite microgels directly by mixing the components in a water-miscible organic solvent.

## Introduction

Colloidal microgels have numerous attractive properties such as defined morphology, high porosity and adjustable dimensions that can respond to changes in temperature, pH and solvent quality, and the ability to act as carriers for drugs, biomolecules, synthetic polymers or inorganic nanocrystals through fluid media. As a consequence, these materials are becoming increasingly important for their potential applications in drug and gene delivery, catalysis, sensing, fabrication of photonic crystals, and separation and purification technologies.<sup>1,2</sup> In such systems, the microgel particles fulfill several important functions, namely a) stabilization and transport of the loaded material in the medium, b) potential controlled release of the load in response to external stimuli, and c) easy recovery by separation from the continuous phase.

Two rather distinct approaches have been taken for loading different substances into microgel particles. The first utilizes

the microgel as a template for *in-situ* preparation of nano-scale materials such as inorganic nanoparticles (NPs). In this case, the nanoparticles are trapped in the microgel interior by hydrophobic forces, hydrogen bonding, or electrostatic interactions. This approach has been realized for both aqueous microgels<sup>2</sup> and microgels dispersed in organic solvents.<sup>3,4</sup> The attractive features of this approach are the effective control of the nanoparticle dimensions within the microgel, and flexibility in control of the nanoparticle loading. The second approach involves filling the microgel by diffusion of pre-formed nanoparticles into the microgel, accompanied by trapping due to the electrostatic interactions or hydrogen bonding with polymer chains.<sup>5</sup> This technique offers some important advantages in terms of the simplicity of the process and independent adjustment of the nanoparticle properties. This approach, however, has been employed primarily in aqueous media and has limited utility for incorporating inorganic nanocrystals synthesized in organic solutions. In both of these approaches, the microgel network serves not only as a container for transporting the nanoparticles, but also as a functional unit that can be attached to substrates or respond to stimuli like changes in temperature or pH. By using the two methods described above, a variety of composite microgel particles have been prepared, containing NPs of conducting polymers,<sup>6</sup> noble metals,<sup>7</sup> metal oxides,<sup>8</sup> metal sulfides,<sup>9</sup> and biominerals.<sup>10</sup> In most cases, the composite microgels preserve the colloidal stability and maintain the stimuli responsiveness of the pure microgels. At the same time, the NPs carried by the composite exhibit the typical physical and chemical properties of nano-materials themselves.

The methods for the preparation of composite microgels described above require the adjustment of the microgel and

<sup>a</sup>Department of Chemistry, University of Toronto, 80 St. George Street, Toronto, M5S 3H6, Ontario, Canada. E-mail: mwinnik@chem.utoronto.ca; gscholes@chem.utoronto.ca; Fax: +1 416-978-0541

<sup>b</sup>The Hefei National Laboratory for Physical Sciences at Microscale, Department of Chemical Physics, University of Science and Technology of China, Hefei, 230026, Anhui, China

<sup>c</sup>Department of Macromolecular Chemistry and Textile Chemistry, Technische Universität Dresden, 01062 Dresden, Germany

<sup>d</sup>Department of Chemistry, The Chinese University of Hong Kong, Shatin, N. T. Hong Kong

† The HTML version of this article has been enhanced with colour images.

‡ Electronic supplementary information (ESI) available: TEM images of the CdSe/TOPO and of the PbS/OA quantum dots. See DOI: 10.1039/b713253k

nanoparticles (or their syntheses) to the nature of the medium, whether water or an organic solvent. The medium in which the composite microgels are formed using these strategies is normally the only medium in which they are stable and can be employed. This limitation can be overcome by the consideration of one important property of the microgel itself, which has not been exploited for microgel–NP composites: the ability of many kinds of microgels to form stable colloidal solutions in solvents of very different polarity. Some authors have noted the nearly universal ability of microgels to form emulsions<sup>11</sup> or colloidal solutions in mixed solvents.<sup>12</sup> Little attention has been paid, however, to the possibility of transferring microgels from water to organic solvents or from organic solvents to aqueous media. Here we show that by selecting solvents that are both miscible with water and also good solvents for the microgel network, one can transfer the microgel from its natural aqueous environment to an organic phase by a solvent exchange process. If this process is reversible and if the microgels retain their stability upon transfer, new designs of composite microgels and their applications become possible.

The method described here for the preparation of inorganic nanoparticle composite microgels is based on the reversible transfer of microgels between water and tetrahydrofuran as the organic solvent. We target semiconductor nanocrystals, often referred to as quantum dots (QDs), which are well known for their unique optical, electrical, magnetic and catalytic properties,<sup>13</sup> recognizing that the best quality QDs are synthesized by a high temperature process in organic media, and have their surface covered with hydrophobic ligands such as trioctylphosphine oxide (TOPO) or oleic acid (OA) that render the NPs insoluble in aqueous solution. On the other hand, many of the applications of these particles, for example in biological systems,<sup>14</sup> require colloidal solutions in water. Our working hypothesis is that appropriately chosen microgels can be synthesized to contain functional groups that can serve as surface ligands for the QDs. These microgels can capture QDs *via* a ligand exchange process in an organic medium, where the QDs form colloidal solutions. Then the composite microgels can be transferred into water, in which the microgel is also able to provide colloidal stability.

In most of our experiments, we employ the imidazole group as our amine-based ligand and examine two different polymer microgel compositions as the carriers: poly(*N*-isopropylacrylamide) (PNIPAM) and poly(*N*-vinylcaprolactam-co-acetoacetyl ethyl methacrylate) (PVCL/AAEM).<sup>14,15</sup> Both types of microgels were synthesized in the presence of different amounts of *N*-vinylimidazole (VIm, 1 to 5 mol%) as the functional co-monomer. We refer to these two types of microgels as PVCL/VIm and PNIPAM/VIm, respectively. The VIm units allow the microgels in THF solution to capture CdSe/TOPO QDs *via* a ligand exchange process.<sup>16,17</sup> We also prepared PNIPAM microgels in the presence of 25 mol% acrylic acid (PNIPAM/AA). Here we wished to explore whether the –COOH groups of these microgels could replace oleic acid from the surface of oleic acid-stabilized PbS (PbS/OA) quantum dots. We show that these microgels, synthesized in water, can be transferred to tetrahydrofuran (THF) solution. When exposed to solutions of CdSe/TOPO in THF, they incorporate the QDs into the microgel network, accompanied by loss of TOPO to the solvent. Afterward, the QD–microgel composites can be transferred to water where they form stable colloidal solutions. We believe that this method opens new possibilities

for the incorporation of a variety of different nanomaterials into microgels and demonstrates the versatility of the microgel particles to provide reversible transport of different materials between organic and aqueous media.

## Experimental

### Materials

The monomers *N*-isopropylacrylamide (NIPAM, 99%, Aldrich), *N*-vinylcaprolactam (VCL, 99%, Aldrich), acetoacetoxyethyl methacrylate (AAEM, 97%, Aldrich), acrylic acid (AA, 99%, Aldrich) and vinylimidazole (VIm, 95%, Aldrich) were used for microgel synthesis after inhibitor removal. The initiators 2,2'-azobis(2-methylpropionamide) dihydrochloride (AMPA, 99%, Aldrich) and potassium persulfate (KPS, 99%, Aldrich) were recrystallized before use. The cross-linker *N,N*-methylene-bisacrylamide (BIS, 99%, Aldrich), the stabilizers cetyltrimethylammonium bromide (CTAB, Aldrich) and sodium dodecyl sulfate (SDS, 99%, Aldrich), and analytical grade tetrahydrofuran (THF, Aldrich) were used as received. Deionized water was obtained from a Millipore Milli-Q water purification system.

The experiment on CdSe quantum dots reported here were carried out with a single sample of trioctylphosphine oxide-passivated QDs (CdSe/TOPO) with a band-edge absorption at 588 nm and a mean core diameter of  $4.5 \pm 0.3$  nm as determined by transmission electron microscopy (TEM). A small number of experiments were carried out with a sample of oleic acid-capped PbS QDs (PbS/OA) with a band-edge absorption at 1108 nm and a mean core diameter of  $3.5 \pm 0.5$  nm as determined by TEM. These samples were prepared by the standard methods described previously.<sup>18,19</sup> TEM images of these two samples are presented in Electronic Supplementary Information (ESI).<sup>†</sup> The nanoparticles were purified by three successive precipitations with methanol followed by redispersion in toluene to remove free ligand from the sample.

### Microgel synthesis

**PNIPAM-based microgels.** Appropriate amounts (see Table 1) of NIPAM, the other monomer (AA or VIm), CTAB and BIS (3 mol%) were dissolved in deionized water in a 100 mL three-neck round-bottom flask equipped with a mechanical stirrer, a reflux condenser, a thermometer and a nitrogen outlet. The monomer mixture was stirred for 30 min at room temperature under a nitrogen purge. The aqueous solution of initiator (KPS for PNIPAM/AA, AMPA for PNIPAM/VIm) was slowly added to the monomer mixture to start the polymerization at 70 °C. The reaction was continued for 4 h. The dispersion was then purified by dialysis against deionized water for a week. The amount of VIm groups in PNIPAM/VIm samples was determined by <sup>1</sup>H NMR with signals at 6.80–7.70 (3H, –NCHNCH–) and 3.50–4.10 (1H, –CH(CH<sub>3</sub>)<sub>2</sub>). The VIm content in PNIPAM/VIm microgels is reported in Table 1.

**PVCL-based microgels.** Appropriate amounts (Table 1) of VCL, AAEM, VIm and BIS (3 mol%) were dissolved in deionized water. A double-wall glass reactor equipped with a mechanical stirrer and a reflux condenser was purged with nitrogen. A solution of the monomers was placed into the reactor and stirred

**Table 1** Amounts of reagents used in the microgel syntheses and the compositions of the microgels

Sample <sup>a</sup>	Monomer <sup>b</sup> /g	AAEM/g	Stabilizer <sup>c</sup> /mg	Comonomer <sup>d</sup> /mg	BIS/mg	Initiator <sup>e</sup> /g	Water/g	$R_h$ <sup>f</sup> /nm	Comonomer ratio <sup>g</sup> [mol%]	Solids content <sup>h</sup> [%]
PNIPAM/AA (25.0%)	0.500	—	10.0	148.0	0.0310	10.0	30	212	~25.0	2.1
PNIPAM/VIm (4.85%)	0.500	—	6.1	20.8	0.0215	10.0	30	113	4.85	1.8
PNIPAM/VIm (2.78%)	0.500	—	6.1	12.5	0.0215	10.0	30	161	2.78	1.7
PNIPAM/VIm (0.87%)	0.500	—	6.1	4.2	0.0215	10.0	30	116	0.87	1.6
PVCL/VIm (4.91%)	1.783	0.3210	—	71.0	0.0600	50.0	150	373	4.91	1.6
PVCL/VIm (2.88%)	1.820	0.3280	—	42.6	0.0600	50.0	150	444	2.88	1.5
PVCL/VIm (0.90%)	1.858	0.3350	—	14.2	0.0600	50.0	150	231	0.90	1.5

<sup>a</sup> We refer to poly(*N*-isopropylacrylamide-co-vinylimidazole) microgel as PNIPAM/VIm, poly(*N*-isopropylacrylamide-co-acrylic acid) microgel as PNIPAM/AA and poly(*N*-vinylcaprolactam-co-acetoacetyl ethyl methacrylate-co-vinylimidazole) microgel as PVCL/VIm. <sup>b</sup> The amount of NIPAM or VCL monomer added for the synthesis of each microgel. <sup>c</sup> The amount of stabilizer (cetyltrimethylammonium bromide (CTAB) for PNIPAM/VIm and sodium dodecyl sulfate (SDS) for PNIPAM/AA synthesis); no stabilizer for PVCL/VIm synthesis. <sup>d</sup> The amount of AA or VIm comonomer for each microgel synthesis. <sup>e</sup> The amount of initiators (potassium persulfate (KPS) for PNIPAM/AA synthesis and 2,2'-azobis(2-methylpropionamide) dihydrochloride (AMPA) for PNIPAM/VIm and PVCL/VIm synthesis). <sup>f</sup> The hydrodynamic radius ( $R_h$ ) determined by 90° DLS in water. <sup>g</sup> The comonomer (AA or VIm) content (in mol%): the VIm content in PNIPAM/VIm microgels was determined by <sup>1</sup>H NMR whereas the VIm content in PVCL/VIm was measured by potentiometric titration.<sup>16</sup> The AA feed ratio was estimated from the amount of monomer added in the synthesis. <sup>h</sup> Determined by gravimetry (freeze drying).

for 1 h at 70 °C with continuous purging with nitrogen. The reaction was continued for 8 h. The dispersion was then purified by dialysis against the deionized water. For these samples, the amount of VIm incorporated into the microgels was determined by potentiometric titration. The results are summarized in Table 1.

### Incorporating QDs into microgels

To prepare QD–microgel hybrid composites, aqueous microgel solutions (0.5 mL, 17.0 mg mL<sup>-1</sup> for PNIPAM/VIm; 16.0 mg mL<sup>-1</sup> for PVCL/VIm) were mixed with THF (2 mL). Each mixture was placed into a dialysis bag (Spectra/Por® Dialysis Membrane, vol = 2.5 mL cm<sup>-1</sup>, molecular weight range: >50 000) and dialyzed against THF for 24 h. The microgel solution in THF obtained (0.5 mL) was mixed with a CdSe/TOPO solution in THF (0.5 mL, 0.4 mg mL<sup>-1</sup>) and then diluted with 2 mL of THF. The mixture was stirred for 24 h at room temperature to ensure complete ligand exchange and incorporation of QD into microgels. The mixture was placed in dialysis bags and dialyzed against THF for 24 h to remove the TOPO molecules replaced by ligand associated with the microgel. Finally the mixture was dialyzed against water for 4 days to ensure complete removal of THF.

Subsequently, we found that the microgel hybrids could be purified and then transferred into water (or other solvents) by centrifugation followed by redispersion in fresh solvent. Once the inorganic particles were incorporated into the microgels, relatively mild centrifugation conditions (6000 rpm for 10 min) were sufficient to sediment the sample.

### Characterization

Hydrodynamic radii ( $R_h$ ) were determined by dynamic light scattering (DLS) using a commercial instrument (ALV/SP-125) equipped with an ALV-5000 multi-tau digital time correlator and a He–Ne laser (Uniphase, 32 mW at  $\lambda = 632.8$  nm) was used. In DLS, the Laplace inversion of each measured intensity–intensity time correlation function  $G^{(2)}(t, q)$  in the self-beating mode can result in a line-width distribution  $G(T)$ . For a pure diffusive relaxation,  $T$  is related to the translational diffusion

coefficient  $D$  by  $\Gamma/q^2 = D$  at  $q \rightarrow 0$  and  $C \rightarrow 0$  or a hydrodynamic radius  $R_h = k_B T / 6\pi\eta D$  with  $k_B$ ,  $T$  and  $\eta$  being the Boltzmann constant, the absolute temperature, and the solvent viscosity, respectively. The samples were all measured at an angle of 90°.

Dark field transmission electron microscopy (TEM) images were taken using a Hitachi HD-2000 STEM instrument operating at 200 kV and 13  $\mu$ A current. Photoluminescence (PL) spectra were taken at room temperature using a SPEX Fluorolog-3 instrument with  $\lambda_{\text{ex}} = 500$  nm. <sup>31</sup>P NMR spectra were obtained at 25 °C with a Varian System 400 NMR. The samples were held in a capillary tube placed inside the 5 mm NMR tube filled with phosphoric acid–D<sub>2</sub>O solution. The QD content of the hybrid microgels were determined by inductively coupled plasma atomic emission spectroscopy (ICP-AES) (Optima 3000 DV equipped with AS-90 autosampler). The instrument was calibrated by using standard aqueous Cd and Se solutions with known concentrations (0.100 mg L<sup>-1</sup> and 4.00 mg L<sup>-1</sup>).

## Results and discussion

Many of the applications of quantum dots in chemistry and biology depend sensitively on the particular ligands bound to the nanoparticle surface. These ligands serve three main functions. First, they passivate the surface to minimize the formation of trap states. Second, they provide colloidal stability and determine the range of solvents with which the QDs are compatible. Finally, for ligand molecules that also contain reactive functional groups, they permit covalent attachment to device components or to biomolecules.

### Ligand exchange

Many research groups have used ligand exchange to modify the surface properties of colloidal nanocrystals. In many cases, one replaces the ligands associated with the particle synthesis (*e.g.*, TOPO from CdSe or oleic acid (OA) from PbS) with other monodentate ligands. Recent reports demonstrate use of multi-dentate ligands such as dendrimers,<sup>20</sup> organic dendrons,<sup>21</sup> and polyelectrolytes<sup>22</sup> to replace ligands bound to the surface of QDs. In many of these systems, amine groups attached to the

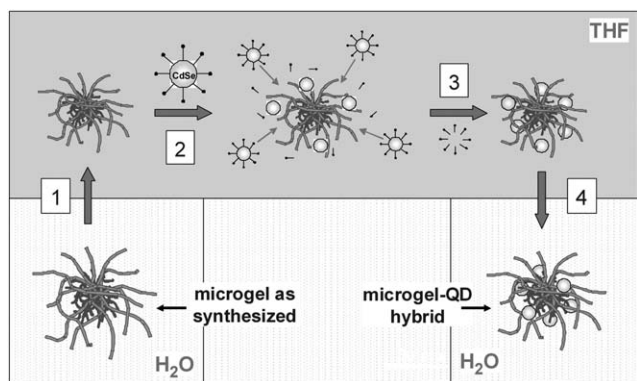


**Fig. 1** Loading CdSe/TOPO nanoparticles (QD) into microgels by the reversible transfer from water to THF and back: 1) transfer of the aqueous microgel to THF by solvent exchange; 2) addition of CdSe/TOPO followed by partial TOPO replacement by imidazole units (ligand exchange) and loading of CdSe into the microgel; 3) dialysis (or centrifugation) in THF to remove free TOPO molecules; 4) transfer of the microgel containing CdSe to the aqueous phase by solvent exchange.

macromolecule serve as the ligands to displace TOPO,<sup>16,17</sup> and this observation played a key role in our experimental design. Here we consider the microgel interior as the carrier of multiple imidazole ligands to replace TOPO from the surface of CdSe quantum dots.

Our general strategy for hybrid microgel synthesis is presented in Fig. 1. In the first step, microgels synthesized in water are transferred to THF by dialysis. Then a THF solution of CdSe/TOPO is added to the microgel dispersion in THF. The diffusion of QDs into the swollen microgel particles is followed by the replacement of TOPO with imidazole groups present in the microgel network. This process leads to essentially irreversible incorporation of the QDs in the microgel and the release of TOPO molecules to the organic solvent. At this point, free TOPO molecules can be removed by dialysis against THF or by centrifugation and re-suspension of the microgels. The composite microgels are easily sedimented by normal centrifugation and can be re-suspended in either THF or any THF-miscible solvent. Thus either by dialysis or by centrifugation–redispersion, the microgel particles loaded with QDs can be transferred back to the aqueous phase. We believe that this method opens new possibilities for the incorporation of different nanomaterials into microgels and demonstrates the versatility of the microgel particles to provide reversible transport of different materials between organic and aqueous media.

We synthesized two different types of microgels. One, based upon poly(*N*-isopropyl acrylamide) (PNIPAM), has an open, porous structure in water at temperatures below the volume phase transition temperature.<sup>14</sup> The second, based upon a copolymer of *N*-vinylcaprolactam (VCL) and acetoacetyl ethyl methacrylate (AAEM), has a core–shell structure.<sup>15</sup> The reactivity ratio mismatch between these two monomers leads to formation of a water-insoluble AAEM-rich core surrounded by a VCL-rich water-swollen corona. Both microgels undergo a collapse transition when their solutions in water are heated above 30–35 °C. The chemical structures of these microgels are presented in Chart 1.

Right angle dynamic light scattering measurements were employed to monitor the effect of loading QDs into microgels

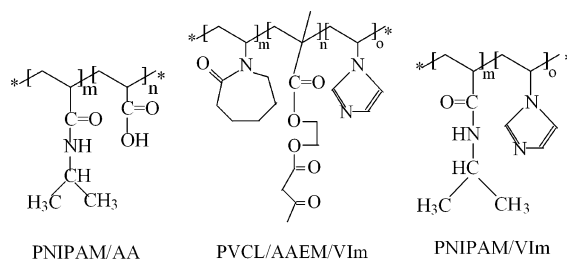


**Chart 1** Chemical structures of the microgel polymers.

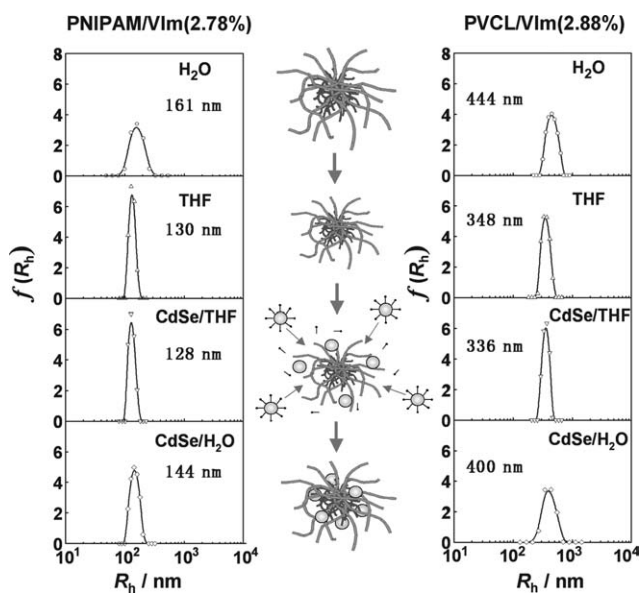


**Fig. 2** Hydrodynamic radius distributions  $f(R_h)$  of different microgel samples following each step of the preparation microgel/QD composite particles. Left-hand column: PNIPAM/VIm (2.78% VIm) at  $1.7 \times 10^{-5}$  g mL<sup>-1</sup> with a final content of 1.1 mg QDs (g polymer)<sup>-1</sup>; right-hand column: PVCL/VIm (2.88% VIm) at  $1.6 \times 10^{-5}$  g mL<sup>-1</sup> with a final content of 1.5 mg QDs (g polymer)<sup>-1</sup>.

on the microgel size and size distribution. Fig. 2 shows size distribution curves of PNIPAM/VIm and PVCL/VIm microgels containing similar amount of VIm units. The four sets of measurements correspond to the four steps of the QDs loading process shown in Fig. 1. Light scattering results presented in Fig. 2 indicate that no aggregation of the microgel particles occurs during any of the steps of the transfer or loading process. The changes in the magnitude of the hydrodynamic radius ( $R_h$ ) indicate that the microgels shrink after transfer to THF due to the elimination of the hydrogen bonds which are responsible for the swelling of the microgels in water below the volume phase transition temperature. The  $R_h$  values, however, are much larger than those of the collapsed microgel particles in water at temperatures above the volume phase transition. Thus the microgels remain extensively swollen by solvent and porous to the penetration of CdSe/TOPO QDs into the interior, where they can interact with the VIm ligands

The experimental data in Fig. 2 indicate that after addition of QDs, the microgel sizes become slightly smaller and the size distribution remains unaltered. After the final transfer of the

CdSe-containing microgel particles into the aqueous phase, the hydrodynamic radii increased. The additional swelling reflects the fact that water is a better solvent for the polymer than THF. Note that the final size of the microgels loaded with QDs in water is smaller than that of the original QD-free samples. Due to the fixation of the QDs in the microgel network, the polymer chains lose some of their mobility and are not able to swell to their original size in water. Such behaviour is reasonable if we consider that every QD can interact with several ligand units, effectively acting as a multifunctional “crosslink” within the microgel particles. The major conclusion drawn from Fig. 2 is that the microgel particles preserve their colloidal stability during solvent exchange followed by QD loading and can be effectively transferred back to the aqueous phase.

To test whether QD uptake by the microgels involves ligand exchange, we used  $^{31}\text{P}$  NMR to monitor the release of free TOPO into the THF solution.<sup>16,17</sup> As reported originally by Emrick and coworkers<sup>16</sup> and confirmed by us,<sup>17</sup>  $^{31}\text{P}$  NMR spectra of purified TOPO-passivated QDs do not exhibit a peak for free TOPO, but this peak appears at 44 ppm as other ligands displace TOPO groups from the QDs surface. This is the result that we obtain here as shown in Fig. 3(a), demonstrating that ligand replacement occurred. We could follow the amount

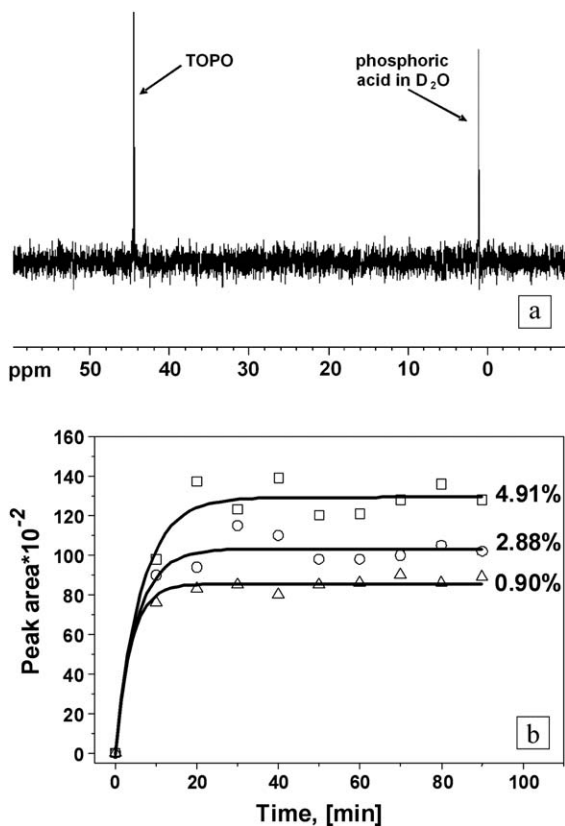


**Fig. 3** a)  $^{31}\text{P}$  NMR spectrum of CdSe (QDs) in THF the presence of PVCL/VIm (4.91%) microgel with phosphoric acid as an internal standard. b) The increase of the 44 ppm  $^{31}\text{P}$  peak area in the  $^{31}\text{P}$  NMR spectrum after mixing solutions of CdSe/TOPO QDs with THF solutions of PVCL/VIm microgels containing different amounts of VIm ligand: 1) 0.90 mol%; 2) 2.88 mol%; 3) 4.91 mol% (the concentrations of QDs and microgel are  $17.8 \text{ mg mL}^{-1}$  and  $16.0 \text{ mg mL}^{-1}$  respectively).

of TOPO released by carrying out the  $^{31}\text{P}$ -NMR experiments in the presence of phosphoric acid as an internal standard (peak at 0 ppm). As shown in Fig. 3(b), the intensity of the TOPO signal increased with the interaction time between the microgel and the QDs, and the integrated area of this peak increased when similar amounts of CdSe/TOPO were added to solutions in THF of microgels containing increasing amounts of imidazole groups. The release of the TOPO molecules appears to be a fast process, and the intensity of the peak reached its maximum level after about 20 min. If the amount of TOPO released is a measure of the amount of QDs incorporated into the microgels, we would conclude that over this range, the amount of QDs taken up by the microgels increases with the pendant ligand content.

### Nature of the hybrid structures

One can control the QD content of the microgel by varying the amount or concentration of QDs added to the microgel solution in THF. In Fig. 4, we compare the amount of CdSe/TOPO taken up by the microgels with the amount of QDs added to the microgel solution in THF.

For these experiments, we employed two microgel samples. The PVCL sample contained 2.88 mol% VIm groups, whereas the PNIPAM sample contained 2.78 mol% VIm. As shown in Fig. 4, we found a nearly linear increase in the QD content of the microgels with an increase in the QD concentration in the THF solution. The QD uptake was far from quantitative, and the QD content, as measured as g (or mg) QDs per g polymer was about a factor of three smaller than that of the solution in which QD incorporation took place. Thus the efficiency of QD loading into the microgels in these experiments is about 30%.

The small difference in QD loading efficiency for the two different microgels is related to their internal structures. Since the diffusion process of the QDs inside microgels is an important step before ligand exchange can take place, the localization of the VIm ligands will play an important role. PVCL/VIm microgels have a core-shell structure that derives from the fact that in the microgel synthesis, AAEM is more reactive than VCL,<sup>15a</sup> leading to a morphology with an AAEM-rich core and a VCL-rich shell.<sup>15b</sup> We imagine that in these microgels, the VIm ligands accumulate in the loosely crosslinked VCL-rich shell, providing a higher local concentration of VIm groups and better access

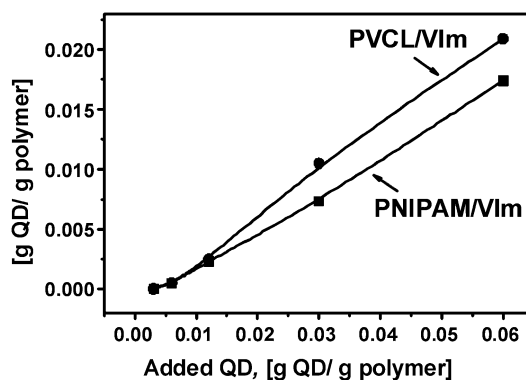


**Fig. 4** The relationship between the added amount of QDs vs. QD content in hybrid microgels for PVCL/VIm (2.88 mol% VIm) and for PNIPAM/VIm (2.78 mol% VIm). The microgel concentration was  $0.6 \text{ mg mL}^{-1}$ .

for the diffusion of QDs to the active sites. In contrast, PNIPAM/VIm microgels have a more uniform structure, with a more random distribution of VIm groups.<sup>1a</sup> Here we speculate that initial binding of CdSe QDs to the microgel structure may hinder subsequent diffusion of particles to the interior of the network. Thus we rationalize how PVCL/VIm microgels with a similar VIm content can load more QDs than PNIPAM/VIm microgels.

Fig. 5 presents dark field STEM images of PVCL and PNIPAM microgels loaded with different amounts of CdSe QDs. In these images for PVCL/VIm hybrid microgels, the QDs appear as bright spots, and one can see that the QDs are relatively uniformly distributed in the corona region of the microgels. In contrast to the PVCL/VIm hybrid microgels, the CdSe QDs distribute uniformly inside the PNIPAM microgels because of a more uniform microgel structure. In addition, one can see some local aggregation of the QDs, particularly at higher levels of loading. This aggregation may take place during drying, but it may also occur during the final dialysis step and microgel

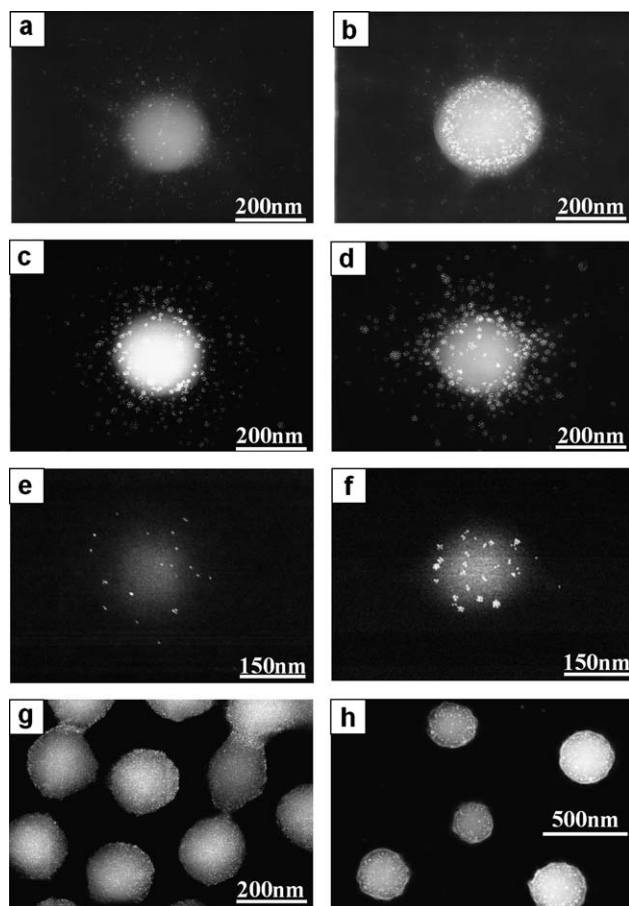


**Fig. 5** (a–d) TEM images of individual PVCL/VIm (2.88%) microgel particles filled with different amounts of CdSe QDs (mg QD (g polymer)<sup>-1</sup>): a) 0.5; b) 2.5; c) 10.5; d) 21.0. In each image, the dense white object is the PAAEM-rich core of the microgel. The QDs are attached to the PVCL/VIm-rich corona. (e, f) TEM images of individual PNIPAM/VIm (2.78%) microgel particles filled with different amounts of CdSe QDs (mg QD (g polymer)<sup>-1</sup>): e) 0.5; f) 2.3. In each image, the QDs are distributed uniformly inside the microgel. (g, h) TEM images of PbS<sub>1108</sub> QDs incorporated into g) PNIPAM/AA (25.0%) microgel particles and h) PVCL/AAEM/VIm (2.88%) microgel particles.

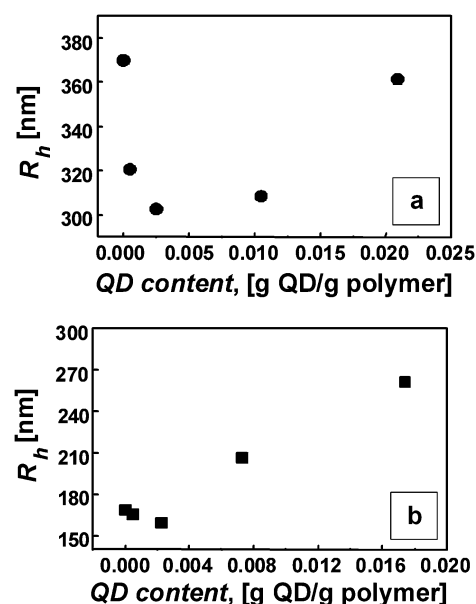


**Fig. 6** The hydrodynamic radii ( $R_h$ ) of (a) PVCL/VIm (2.88%) hybrid microgels and (b) PNIPAAm/VIm (2.78%) hybrid microgels as a function of CdSe QD content.

transfer to the aqueous phase. TOPO groups remaining on the QDs surface will render portions of the surface hydrophobic,<sup>17b</sup> and aggregation would provide a means to minimize the total surface area in contact with water molecules. When the QD content of the microgel is low, the QDs are well separated by hydrophilic polymer chains, and no aggregation occurs.

At higher loading (up to 5 mg (g polymer)<sup>-1</sup>), the hydrodynamic radii decrease substantially, as shown in Fig. 6. A greater extent of cross-linking (and perhaps hydrophobic interactions between the QDs) restricts the swelling of the microgels. Even higher levels of loading (above 20 mg (g polymer)<sup>-1</sup>) lead to a decrease in colloidal stability as inferred from the increase in  $R_h$  values measured by DLS, accompanied by an increase in the breadth of the  $R_h$  distribution. This increase is almost certainly due to the formation of dimers and small aggregates of microgels in the aqueous solution. In this case, hydrophobic attraction forces will dominate, leading to formation of aggregates. This result leads to the conclusion that at high QD loadings, the QDs accumulate preferably in the microgel shell reducing the efficiency of the steric stabilization provided by the hydrophilic microgel outer layer.

As a test of the generality of this approach, we carried out a few additional experiments with a sample of oleic acid-stabilized PbS quantum dots prepared by the method of Hines and Scholes.<sup>19</sup> These nanocrystals (PbS<sub>1108</sub>) have a mean diameter of *ca.* 3.5 ± 0.5 nm (TEM) and an absorption peak at 1108 nm (see Electronic Supplementary Information (ESI)†). Solutions of these QDs in THF could be captured effectively by the PVCL/AAEM/VIm microgels, and even more effectively by the carboxyl groups of PNIPAM/AA microgels. Both samples could then be transferred into water. Dark field TEM images of these composite particles are shown in Fig. 5g and h. We can see that all the PbS QDs are captured in the AAEM core of PVCL/AAEM/VIm microgels, which suggests that the β-ketoester groups of AAEM rather than the VIm groups displace oleic acid on PbS QDs. We conclude that

this microgel exchange method works well for a variety of QDs insoluble in aqueous solution.

### Temperature sensitivity

The microgels loaded with QDs preserve their temperature-sensitive properties. Fig. 7a shows the variation of hydrodynamic radius with temperature for two PVCL/VIm(2.88%) microgel samples. The microgel sample containing QDs exhibits a similar temperature-response behavior to that of the as-prepared microgel. Increase of the temperature induces collapse of the microgel due to the destruction of the hydrogen bonds that oppose the hydrophobic attraction forces between polymer chains. Both the original microgel and the microgel filled with QDs collapse to similar size, which indicates that QDs do not influence strongly the mobility of the polymer chains above volume phase transition temperature. A similar response is found for a PNIPAM/VIm microgel sample at a similar QDs loading. The volume phase transition temperature is shifted to lower temperatures due to the hydrophobic nature of the QDs. In this case, the QDs provoke faster deswelling of the microgel by enhancing the hydrophobic attraction forces within microgel.

After transfer to the microgel, the CdSe QDs remain photoluminescent (PL). As seen in Fig. 7b, the PVCL/VIm/CdSe composite in THF has a nearly identical PL spectrum to that of CdSe/TOPO. The emission in water is substantially weaker, and blue shifted,<sup>23</sup> as is shown in Fig. 7b for PVCL/VIm/CdSe. The dramatic reduction of the quantum yield of QDs occurs not during the ligand exchange step but during microgel transfer to the aqueous phase. (It is difficult to compare quantum yields because light scattering from the microgel composite masks the

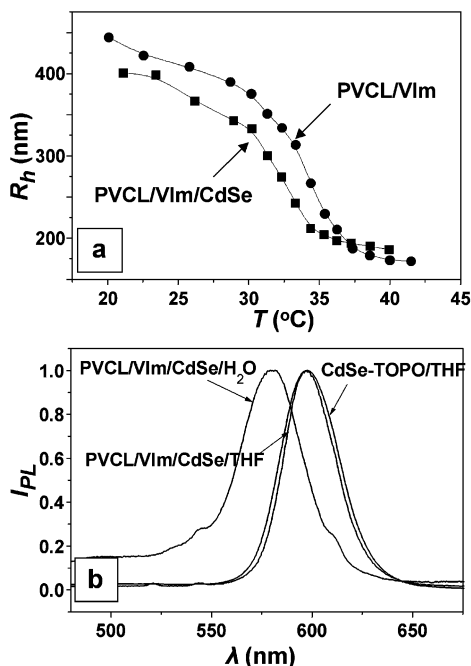


**Fig. 7** a) Temperature dependence of  $R_h$  for PVCL/VIm (2.88%) microgel in water with (10.5 mg QD (g polymer)<sup>-1</sup>) and without QDs. b) normalized emission spectra of CdSe/TOPO in THF and CdSe/PVCL/VIm (2.88%) hybrid microgel (10.5 mg QD (g polymer)<sup>-1</sup>) in THF and in water.

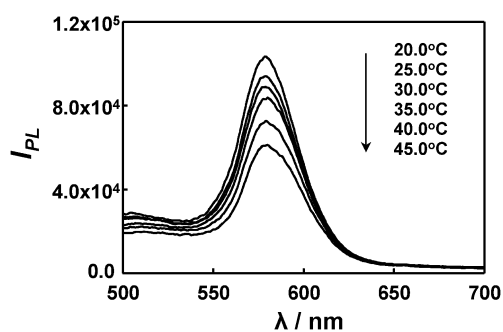


**Fig. 8** Temperature dependence of emission spectra of CdSe/PVCL/VIm (2.88%) hybrid microgel (10.5 mg QD (g polymer)<sup>-1</sup>) in water (0.2 mg mL<sup>-1</sup>).

UV-Vis absorption spectrum of the QDs.) A similar reduction in PL intensity has been reported for CdSe nanoparticles coated with poly(*N,N*-dimethylaminoethyl methacrylate), following transfer from toluene to water.<sup>17b</sup> Fig. 8 shows the temperature dependence of the PL emission spectrum of PVCL/VIm/CdSe composite (10.5 mg QD (g polymer)<sup>-1</sup>) in water. The PL intensities decreased as the temperature increased,<sup>24</sup> and the effect was reversible. A slight blue shift of the PL maximum wavelength associated with small changes in peak shape accompanied this increase in temperature.

### Conclusions

We demonstrate a new approach for the preparation of hybrid microgels containing inorganic nanoparticles, using TOPO-passivated CdSe QDs and oleic acid capped PbS QDs as examples. In this method, nanoparticles prepared by traditional high temperature methods in organic solvents, and covered with a layer of organic ligands at their surface, are incorporated into the microgel in a water-miscible organic solvent such as THF. Functional groups introduced as part of the microgel structure exchange with ligands from the nanoparticle synthesis, and the nanoparticles become irreversibly incorporated into the polymer network. These hybrid structures can then be transferred back to water.

Our experimental results demonstrate that the microgels, synthesized in water, retained their colloidal stability during the transfer from water to THF; and the QD-microgel hybrid particles retained their colloidal stability in THF and during transfer from THF to water. We were able to show that QD binding to the microgel took place by a ligand exchange process. This approach worked well for polymer microgels of two different compositions, one based upon PNIPAM, and the other on a copolymer of AAEM with *N*-vinylcaprolactam. Small differences in behavior were noted and attributed to the different internal morphologies of these microgels. The QDs incorporated into the microgels remained photoluminescent, both in THF and in water. The hybrid microgels retained their temperature-sensitive properties in aqueous solution, but the presence of the QDs shifted the volume phase transition to lower temperatures. We believe that this new approach can be used to incorporate a broad range of nanoparticles into microgels and can also lead to the design of novel multifunctional materials.

## Acknowledgements

The authors thank NSERC Canada for their support of this research. We also thank Karolina Fritz for a kind gift of the PbS QD sample.

## References

- (a) R. Pelton, *Adv. Colloid Interface Sci.*, 2000, **85**, 1; (b) S. Nayak and L. A. Lyon, *Angew. Chem., Int. Ed.*, 2005, **44**, 7686; (c) N. A. Peppas, J. Z. Hilt, A. Khademhosseini and R. Langer, *Adv. Mater.*, 2006, **18**, 1345; (d) M. Das, H. Zhang and E. Kumacheva, *Annu. Rev. Mater. Res.*, 2006, **36**, 117.
- J. Zhang, S. Xu and E. Kumacheva, *J. Am. Chem. Soc.*, 2004, **126**, 7908.
- M. Antonietti, F. Grohn, J. Hartmann and L. Bronstein, *Angew. Chem., Int. Ed. Engl.*, 1997, **36**, 2080.
- A. Biffis, N. Orlandi and B. Corain, *Adv. Mater.*, 2003, **15**, 1551.
- (a) I. Gorelikov, L. M. Field and E. Kumacheva, *J. Am. Chem. Soc.*, 2004, **126**, 15938; (b) M. Kuang, D. Yang, H. Bao, M. Gao, H. Möhwald and M. Jiang, *Adv. Mater.*, 2005, **17**, 267; (c) Y. Gong, M. Gao, D. Wang and H. Möhwald, *Chem. Mater.*, 2005, **17**, 2648.
- (a) J. Mrkic and B. R. Saunders, *J. Colloid Interface Sci.*, 2000, **222**, 75; (b) A. Pich, Y. Lu, H. P. Adler, T. Schmidt and K. Arndt, *Polymer*, 2002, **43**, 5723; (c) A. Pich, Y. Lu, V. Boyko, K.-F. Arndt and H.-J. P. Adler, *Polymer*, 2003, **44**, 7651; (d) A. Pich, Y. Lu, V. Boyko, S. Richter, K. Arndt and H. P. Adler, *Polymer*, 2004, **45**, 1079; (e) E. Lopez-Cabarcos, D. Mecerreyes, B. Sierra-Martin, M. S. Romero-Cano, P. Strunz and A. Fernandez-Barbero, *Phys. Chem. Chem. Phys.*, 2004, **6**, 1396; (f) J. Rubio Retama, E. Lopez Cabarcos, D. Mecerreyes and B. Lopez-Ruiz, *Biosens. Bioelectron.*, 2004, **20**, 1111.
- (a) G. Sharma and M. Ballauff, *Macromol. Rapid Commun.*, 2004, **25**, 547; (b) Y. Mei, G. Sharma, Y. Lu, M. Ballauff, M. Drechsler, T. Irrgang and R. Kempe, *Langmuir*, 2005, **21**, 12229; (c) Y. Lu, Y. Mei, M. Drechsler and M. Ballauff, *Angew. Chem., Int. Ed.*, 2006, **45**, 813; (d) D. Suzuki and H. Kawaguchi, *Langmuir*, 2005, **21**, 12016; (e) J. Zhang, S. Xu and E. Kumacheva, *Adv. Mater.*, 2005, **17**, 2336; (f) A. Pich, A. Karak, Y. Lu, A. Ghosh and H. J. P. Adler, *Macromol. Rapid Commun.*, 2006, **27**, 344; (g) A. Biffis, N. Orlandi and B. Corain, *Adv. Mater.*, 2003, **15**, 1551.
- (a) M. Gao, X. Peng and J. Shen, *Thin Solid Films*, 1994, **248**, 106; (b) C. Menager, O. Sandre, J. Mangili and V. Cabuil, *Polymer*, 2004, **45**, 2475.
- (a) C. Bai, Y. Fang, Y. Zhang and B. Chen, *Langmuir*, 2004, **20**, 263; (b) A. Pich, J. Hain, Y. Lu, V. Boyko, Y. Prots and H. Adler, *Macromolecules*, 2005, **38**, 6610.
- (a) N. Nassif, N. Gehrke, N. Pinna, N. Shirshova, K. Tauer, M. Antonietti and H. Cölfen, *Angew. Chem.*, 2005, **117**, 6158; (b) G. Zhang, D. Wang, Z. Gu, J. Hartmann and H. Möhwald, *Chem. Mater.*, 2005, **17**, 5268; (c) G. Zhang, D. Wang, Z. Gu and H. Möhwald, *Langmuir*, 2005, **21**, 9143.
- (a) S. Fujii, E. S. Read, B. P. Binks and S. P. Armes, *Adv. Mater.*, 2005, **17**, 1014; (b) T. Ngai, S. H. Behrens and H. Auweter, *Chem. Commun.*, 2005, 331; (c) T. Ngai, S. H. Behrens and H. Auweter, *Macromolecules*, 2006, **39**, 8171; (d) S. Fujii, S. P. Armes, B. P. Binks and R. Murakami, *Langmuir*, 2006, **22**, 6818; (e) A. Y. C. Koh and B. R. Saunders, *Langmuir*, 2005, **21**, 6734.
- H. M. Crowther and B. Vincent, *Colloid Polym. Sci.*, 1998, **276**, 46.
- (a) M. P. Bruchez, M. Moronne, P. Gin, S. Weiss and A. P. Alivisatos, *Science*, 1998, **281**, 2013; (b) W. C. W. Chan and S. Nie, *Science*, 1998, **281**, 2016; (c) X. Michalet, F. F. Pinaud, L. A. Bentolila, J. M. Tsay, S. Doose, J. J. Li, G. Sundaresan, A. M. Wu, S. S. Gambhir and S. Weiss, *Science*, 2005, **307**, 538; (d) T. M. Jovin, *Nat. Biotechnol.*, 2003, **21**, 32; (e) I. L. Medintz, H. T. Uyeda, E. R. Goldman and H. Mattoussi, *Nat. Mater.*, 2005, **4**, 435; (f) J. M. Klostranec and W. C. W. Chan, *Adv. Mater.*, 2006, **18**, 1953.
- (a) H. Weller, *Angew. Chem., Int. Ed. Engl.*, 1993, **32**, 41; (b) A. P. Alivisatos, *J. Phys. Chem.*, 1996, **100**, 13226.
- (a) V. Boyko, A. Pich, Y. Lu, S. Richter, K.-F. Arndt and H.-J. Adler, *Polymer*, 2003, **44/25**, 7821; (b) A. Pich, A. Teissier, V. Boyko, Y. Lu and H.-J. P. Adler, *Macromolecules*, 2006, **39**, 7701.
- (a) H. Skaff and T. Emrick, *Chem. Commun.*, 2003, 52; (b) K. Sill and T. Emrick, *Chem. Mater.*, 2004, **16**, 1240.
- (a) X.-S. Wang, T. E. Dykstra, X. Lou, M. R. Salvador, I. Manners, G. D. Scholes and M. A. Winnik, *J. Am. Chem. Soc.*, 2004, **126**, 7784; (b) M. Wang, J. K. Oh, T. E. Dykstra, X. Lou, G. D. Scholes and M. A. Winnik, *Macromolecules*, 2006, **39**, 3664; (c) M. Wang, T. E. Dykstra, X. Lou, M. R. Salvador, G. D. Scholes and M. A. Winnik, *Angew. Chem., Int. Ed.*, 2006, **45**, 2221.
- C. B. Murray, D. J. Norris and M. G. Bawendi, *J. Am. Chem. Soc.*, 1993, **115**, 8706–8715.
- M. A. Hines and G. D. Scholes, *Adv. Mater.*, 2003, **15**, 1844.
- C. Zhang, S. O'Brien and L. Balogh, *J. Phys. Chem. B*, 2002, **106**, 10316.
- Y. A. Wang, J. J. Li, H. Chen and W. Peng, *J. Am. Chem. Soc.*, 2002, **124**, 2293.
- I. Potapova, R. Mruk, S. Prehl, R. Zentel, T. Basche and A. Mews, *J. Am. Chem. Soc.*, 2003, **125**, 320.
- Y. Zhang, J. He, P. N. Wang, J. Y. Chen, Z. J. Lu, D. R. Lu, J. Guo, C. C. Wang and W. Y. Yang, *J. Am. Chem. Soc.*, 2006, **128**, 13396.
- J. Li, X. Hong, Y. Liu, D. Li, Y. Wang, J. Li, Y. Bai and T. Li, *Adv. Mater.*, 2005, **17**, 163.